Computational Mechanistic Study on N-Nitrosation Reaction of Secondary Amines

Meire Y. Kawamura
Lhasa Limited
David J. Ponting
Lhasa Limited
Chris G. Barber
Lhasa Limited
Michael J. Burns
michael.burns@lhasalimited.org
Lhasa Limited

Research Article

Keywords: nitrosamine, secondary amine, dinitrogen trioxide, density functional theory (DFT), drug product

Posted Date: July 25th, 2025

DOI: https://doi.org/10.21203/rs.3.rs-7158176/v1

Additional Declarations: No competing interests reported.

Version of Record: A version of this preprint was published at Journal of Molecular Modeling on October 16th, 2025. See the published version at https://doi.org/10.1007/s00894-025-06520-7.

Title: Computational Mechanistic Study on *N*-Nitrosation Reaction of Secondary Amines

Authors: Meire Y. Kawamura[1], David J. Ponting[1], Chris G. Barber[1], Michael J. Burns[1*]

[1]Lhasa Limited, Granary Wharf House, 2 Canal Wharf, Leeds, United Kingdom

*Corresponding author

E-mail address: michael.burns@lhasalimited.org

ORCID:

M.Y.K.: 0009-0003-0214-1683

D.J.P.: 0000-0001-6840-2629

C.G.B.: 0000-0003-4220-1137

M.J.B.: 0000-0002-5569-1270

Abstract

Context

The presence of potentially carcinogenic nitrosamines in drugs has been a worldwide concern, driving strategies to control or mitigate their formation to protect patient health. Understanding the critical factors for *N*-nitrosation, such as mechanisms and energy barriers, enhances confidence in decision-making for the risk assessment of nitrosamine formation. Evaluation of structural impact of amines on the *N*-nitrosation rate in the presence of nitrites and acidic media is of great interest to pharmaceutical companies assessing the risk of nitrosamine drug substance-related impurities. A range of secondary amines were explored using DFT calculations to assess the impact of electronic and steric effects on activation energy. *Asym*-N_2O_3 was selected as the nitrosating agent since its reaction was shown to be favourable following screening of pathways employing nitrosyl chloride, nitric acid, *asym*-N_2O_3, *sym*-N_2O_3 and *trans-cis*-N_2O_3. The relatively low activation energies obtained for all amines indicate the reaction is very likely to occur if the reactive components encounter, even for amines with sterically hindered and electron-withdrawing groups. Understanding the interaction of amine and nitrosating agent is therefore the defining factor in the risk of formation of more complex nitrosamines within drugs. Furthermore, the amine pK_a plays an important role in the relative reaction rates and should also be considered in risk evaluations.

Methods

Calculations were performed using Gaussian-16 program. The B3LYP-D3/def2-TZVP level of theory was applied for structure optimizations. The IEF-PCM implicit model was used for solvent effect. Intrinsic reaction coordinate calculations were carried out to connect the transition state with the associated minimum.

Keywords

nitrosamine, secondary amine, dinitrogen trioxide, density functional theory (DFT), drug product

Introduction

The formation of *N*-nitrosamines in drug products has received considerable attention after the detection of *N*-nitrosodimethylamine (NDMA) and *N*-nitrosodiethylamine (NDEA) in sartans [1]. Further investigations led to the discovery of *N*-nitrosamines in other pharmaceutical products such as metformin, ranitidine and varenicline [2, 3]. Whilst initial concerns related to the presence of small highly potent nitrosamines associated with drug substance synthesis, later the focus has transitioned to nitrosamine derivatives of larger more complex nitrosamines, commonly referred to as Nitrosamine Drug Substance-Related Impurities (NDSRIs) [4–6]. The presence of these substances within pharmaceutical compounds has been subject to rigorous and evolving regulations from worldwide health authorities [7–9], where the risk assessment for the presence of *N*-nitrosamines in different stages of the drug manufacture and during storage has been necessitated. A key aspect of the assessment is understanding the potential for nitrosamine formation, particularly of NDSRIs, where long-term exposure to low levels of nitrites in excipients can create a favourable environment for nitrosation. Increased understanding of the mechanism of *N*-nitrosation offers an avenue to assess the potential for nitrosation and thereby contribute to strategies to predict, mitigate or control *N*-nitrosamine formation.

There are different routes for the formation of *N*-nitrosamines but the predominant pathway in drug products is the co-presence of amines and nitrite impurities. Deactivated trialkyl amines are significantly less reactive than secondary amines (1000-times lower) [10], whereas primary amines generate unstable *N*-nitrosamines that readily degrade [11]. Secondary amines can therefore be considered the main risk of patient exposure. A nitrite requires the presence of acid or a suitable catalyst (e.g. formaldehyde) to generate the active nitrosating species [12, 13]. In acidic conditions, it is believed that the source of the nitrosation agents can be dinitrogen trioxide (N_2O_3), nitrosyl chloride (ClNO), nitrosonium ion (NO^+) or protonated nitrous acid ($H_2NO_2^+$) depending on the precise reaction conditions [14] (**Figure *1***). Kinetic experiments have shown the species that would be more relevant for nitrosation within pharmaceutical formulations are either dinitrogen trioxide (N_2O_3) or nitrosyl chloride (ClNO) [15]. Three main isomers for N_2O_3 have been reported in the literature [16, 17], asymmetric N_2O_3 (*asym*- N_2O_3), symmetric N_2O_3 (*sym*- N_2O_3), and *trans-cis* N_2O_3. The most stable isomer is *asym*-N_2O_3 and is therefore expected to be the predominant species [18, 19].

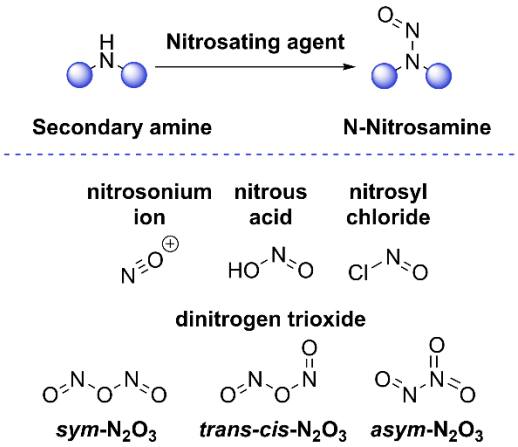

Figure 1. Potential nitrosating agents generated when nitrites are in acidic conditions.

Whilst the reaction of secondary amines with nitrites has been extensively studied kinetically [15, 20–23], to date there is still a lack of understanding about how electronic and steric effects influence the reaction. A powerful way to assess these properties is through computational (simulation) approaches, which provides the detailed examination of reaction pathways. Density Functional Theory (DFT) is one of the most widely used quantum mechanical methods for studying small organic molecules and reaction mechanisms. DFT calculations can provide insights into reaction pathways by calculating reactant, product and transition state energies, enabling the prediction of reactivity trends based on electronic and steric factors. Computational studies complement experimental data and help explain the fundamental factors governing chemical reactivity by calculating potential energy surfaces, activation barriers, transition state geometries, and electronic properties.

Herein, we utilise DFT to assess the *N*-nitrosation of a variety of simple secondary amines via nitrosation agents which may be generated from nitrites in acidic media. The aim of which is to further our understanding of the formation of nitrosamines to enable risk assessments for nitrosamine formation of NDSRIs and other small molecule secondary amines, considering the local environment of the nitrogen.

Computational methods

DFT calculations were performed using Gaussian-16 [24] with an ultrafine integration grid. All structures were fully optimized with the B3LYP [25–27] functional using the def2-TZVP [28] basis set and including empirical dispersion corrections using the Grimme D3 (GD3) method [29]. The IEF-PCM [30, 31] implicit model was used to include solvent effects. Vibrational frequency calculations at 298.15 K (1 atm) were used to confirm that stationary points were either minima or first-order saddle points on the potential energy surface. Intrinsic reaction coordinate (IRC) calculations were performed to confirm that each transition state (TS) connects reagents and products with the corresponding transition states. Structures were visualized with GaussView 6.1.1. [32] and CYLview [33]. Graphs were created using Plotly Chart Studio and Canva.

Results and discussion

Structures of nitrosating agents and transition state energies. DFT calculations were performed to study the reaction mechanism involved in nitrosamine formation. Nitrosyl chloride, nitric acid and the three isomers of dinitrogen trioxide (*asym*- N_2O_3, *sym*- N_2O_3 and *trans-cis* N_2O_3) were individually evaluated for the *N*-nitrosation of dimethylamine (DMA). Transition states were subsequently identified for each of these isomeric forms, as well as NOCl and HNO_2 (**Scheme 1**).

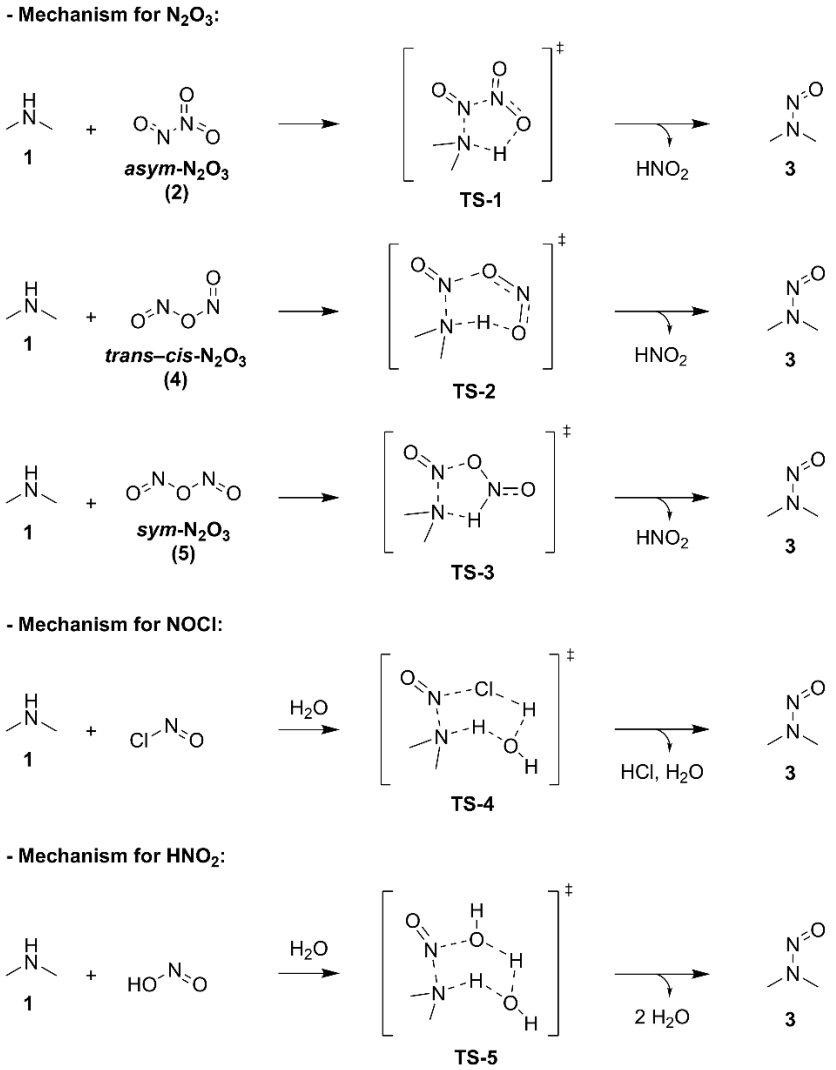

Scheme 1. Reaction mechanism for *N*-nitrosation of DMA by nitrosyl chloride, nitric acid and dinitrogen trioxide.

The optimized structural geometries for reactants, products and transition states for the pathways displayed in **Scheme 1** were calculated to obtain the most favourable mechanism to consider in our evaluation of reactivity of secondary amines.

The energy profiles for the nitrosation of DMA by *asym*-N_2O_3, *trans*-N_2O_3 and *sym*-N_2O_3 are represented in **Figure *2***. The energies are relative to the energy of *asym*-N_2O_3 + DMA, as they demonstrated to be the most stable reactants. All three transition states for the N_2O_3 isomers were

calculated. Overall, the transition state for *asym*-N_2O_3, **TS-1** (3.0 kcal mol^{-1}) presented the lowest relative energy, followed by *trans*-N_2O_3, **TS-2** (3.2 kcal mol^{-1}) and then *sym*-N_2O_3, **TS-3** (5.4 kcal mol^{-1}). In terms of the barrier, the process for *trans*-N_2O_3 (**TS-2**, -3.1 kcal mol^{-1}) and *sym*-N_2O_3 (**TS-3**, -0.3 kcal mol^{-1}) are barrierless which was already reported previously [18]. However, when the pre-complexes **PC-1** (-1.6 kcal mol^{-1}), **PC-2** (1.0 kcal mol^{-1}) and **PC-3** (3.5 kcal mol^{-1}) are considered, the N_2O_3 structures are stabilized by interaction with DMA lowering the reactants energies (**Figure 2**). As a result, a barrier of 4.6 kcal mol^{-1}, 2.2 kcal mol^{-1} and 1.9 kcal mol^{-1} for **TS-1**, **TS-2** and **TS-3**, is calculated.

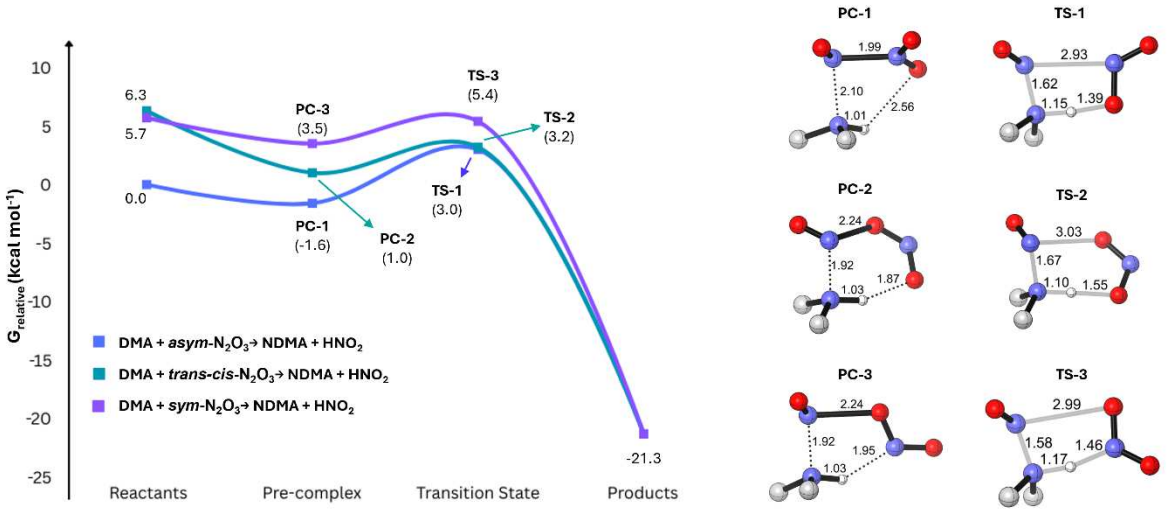

Figure 2. Gibbs free energy (G) profiles of the *N*-nitrosation of DMA by N_2O_3 isomers at the B3LYP-D3/def2-TZVP (IEF-PCM:water) level of theory. Bond lengths are shown in Å.

Despite the higher barrier existing for the pathway with the *asym*-N_2O_3 isomer, the process is still very energetically favourable and since the reactants DMA + *asym*-N_2O_3 are more stable relative to the other isomers with DMA, *asym*-N_2O_3 was considered as the primary nitrosation agent for further investigations [18, 34, 35]. Moreover, the energy for the interconversion among the isomers is very high and unlikely to occur within the drug product processing [18].

The energy profiles considering NOCl and HNO_2 as nitrosating agent were also calculated (**Figure *3***). The energies showed in the **Figure *3*** are relative to the respective reactants. The transition states calculated for both **TS-4** and **TS-5** are water assisted 6-membered systems. Starting with HNO_2, as expected, the results demonstrated a very high energy barrier (24.8 kcal mol^{-1}) while the nitrosyl chloride showed a much lower energy barrier (4.7 kcal mol^{-1}) than HNO_2 and comparable but still higher than the barrier of *asym*-N_2O_3 isomer (3.0 kcal mol^{-1}).

Attempts to obtain the transition state of direct nitrosation of DMA by the nitrosonium ion were made; however, no saddle point was found. The structure of the transition state appears to be too unstable and all the simulations converged to the structure of the product NDMA.

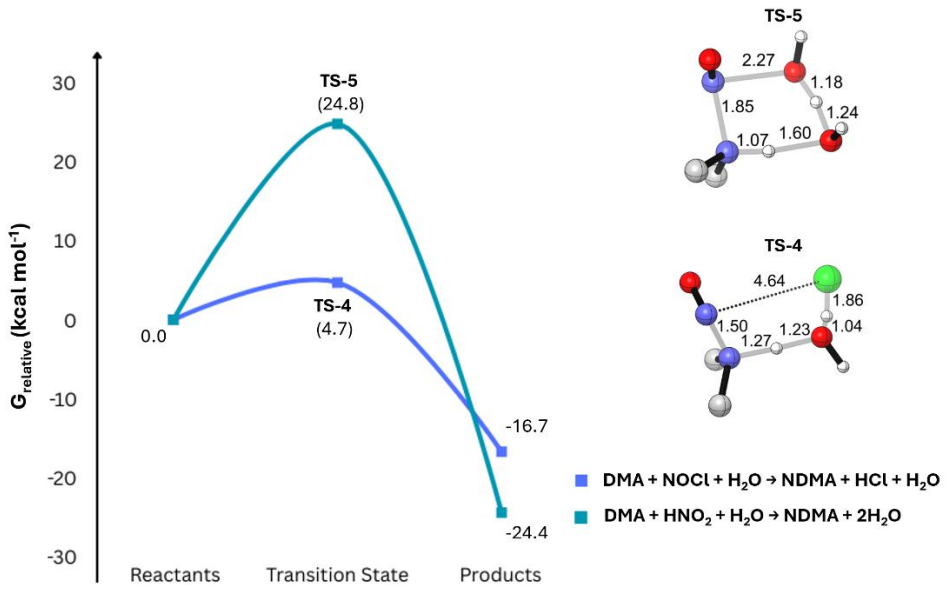

Figure 3. Gibbs free energy (G) profile of the *N*-nitrosation of DMA by HNO_2 and NOCl at the B3LYP-D3/def2-TZVP (IEF-PCM:water) level of theory. Bond lengths are shown in Å.

Steric and electronic effects of *N*-nitrosation of secondary amines by *asym*-N_2O_3. The activation and free energies for the *N*-nitrosation reaction of 24 secondary amines by *asym*-N_2O_3 were evaluated. The selection of secondary amines was undertaken to investigate the impact of steric hindrance and electronic factors, while maintaining small molecular size to keep computational time reasonable.

Acyclic amines, heterocyclic amines and aromatic amines were all incorporated into the study (**Figure 7**). Optimization of reactants, products and transition states structures were performed for all amines. All the transition state geometries found presented a similar 5-membered cyclic transition states as **TS-1** (**Figure 4, Figure 5 and Figure 6**).

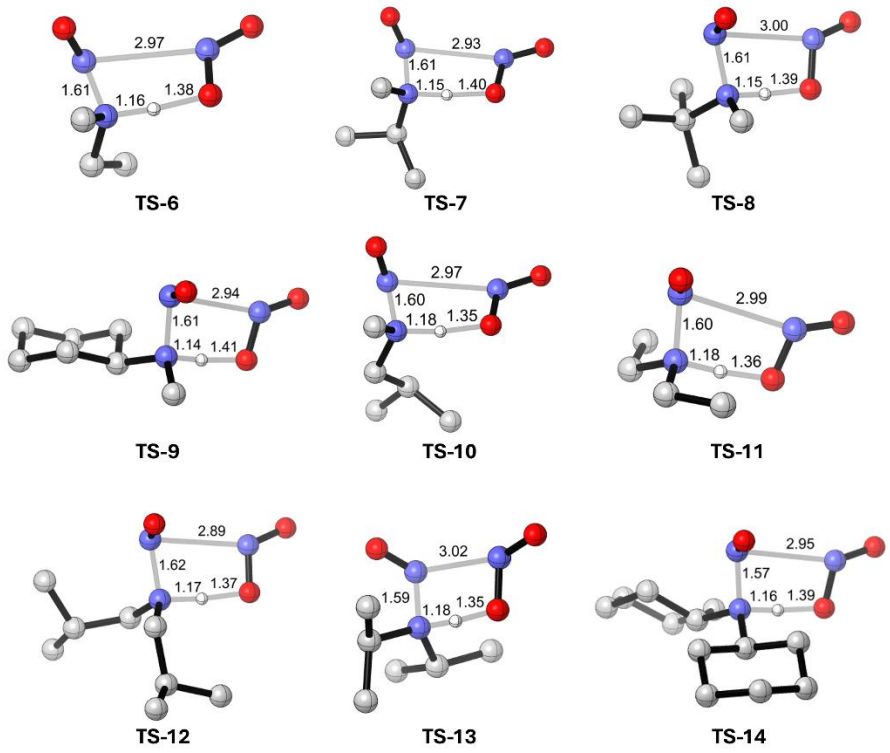

Figure 4. Geometries of transition states for **TS-6** to **TS-14** related to acyclic amines **6**-**14.**

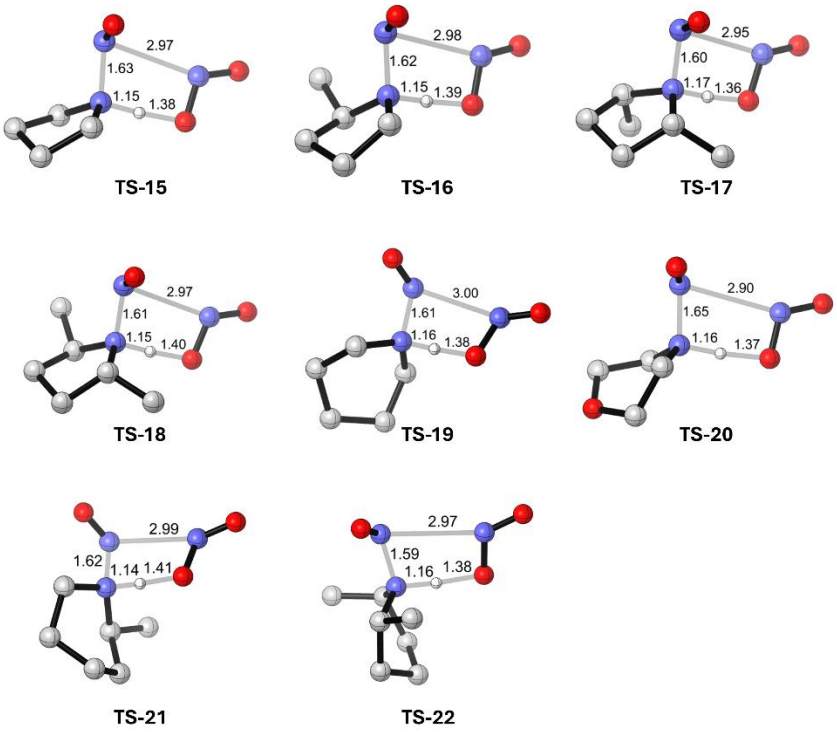

Figure 5. Geometries of transition states for **TS-15** to **TS-22** related to heterocyclic amines **15**-**22.**

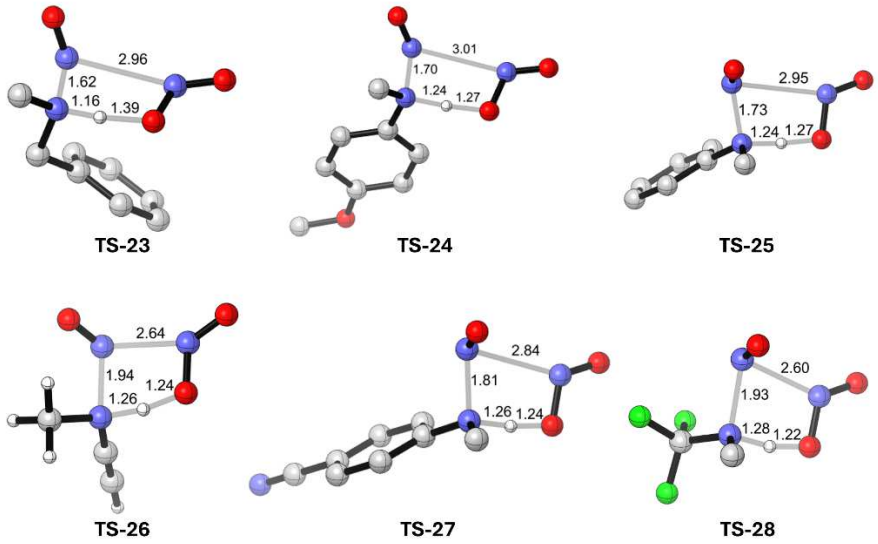

Figure 6. Geometries of transition states for **TS-23** to **TS-28** related amines **23**-**28.**

The results for acyclic amines **1, 6-14** demonstrated that steric effects influence their reactivities. Among the amines studied, DMA (**1**) exhibited the lowest energy barrier at 2.97 kcal mol^{-1} and dicyclohexylamine (**14**) had the highest at 9.58 kcal mol^{-1}. The results for the heterocyclic amines **15-22** showed that structures with the pyrrolidine core present lower reactivity than piperidines. Pyrrolidine (**15**) having the lowest activation energy at 1.97 kcal mol^{-1}, whereas 2,6-dimethylpiperidine (**22**) had the highest at 9.53 kcal mol^{-1}. The presence of an additional heteroatom in the ring influenced the energy barrier, with morpholine (**20**) showing a higher activation energy (9.18 kcal mol^{-1}) compared to piperidine (**19**) (6.61 kcal mol^{-1}).

The free energy across all the alkyl amines studied (acyclic and heterocyclic amine) was in a range of -21.49 to -15.38 kcal mol^{-1}, demonstrating that the reaction is thermodynamically highly favourable. The low energy barrier for *N*-nitrosation indicates the reaction is likely to occur easily, although at different rates due to the different activation energies. Furthermore, the high reactivities of the amines indicates an encounter-controlled reaction. In such cases, the reaction is primarily governed by the diffusion of the reactants rather than the reactivity of the amine. This observation aligns with previous findings from experimental kinetics studies [22], which support our results.

Considering the aromatic amines **24**, **25** and **27**, the energy barrier clearly decreases in the presence of an electron donating group and increases with an electron withdrawing group in the aromatic ring, as demonstrated by the barrier decreasing across the series of 4-cyano-*N*-methylaniline **27** (16.10 kcal mol^{-1}), *N*-methylaniline **25** (10.34 kcal mol^{-1}) and 4-methoxy-*N*-methylaniline **24** (7.15 kcal mol^{-1}). Additionally, amines **23**, **26** and **28** were selected to evaluate the electronic effects of the groups directly attached to the nitrogen. The activated amine **23** demonstrated to be more reactive (5.25 kcal mol^{-1}) and the deactivated amines **26** and **28** showed higher barriers at 13.43 kcal mol^{-1} and 18.76 kcal mol^{-1}, respectively. Lastly, concerning to free energy, the amines **23-28** are thermodynamically favourable with free energies from -17.87 kcal mol^{-1} to -3.77 kcal mol^{-1}, however to a lesser degree than the aliphatic amines.

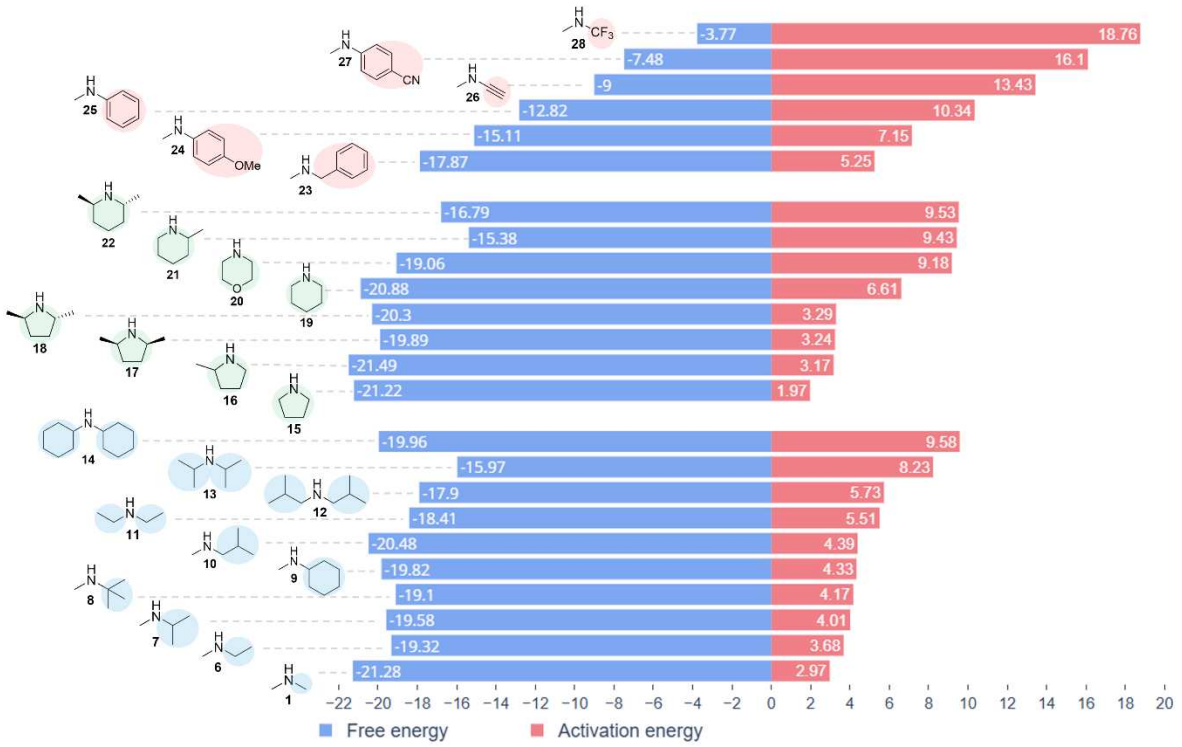

Figure 7. Calculated free energy and activation energy in kcal mol^{-1} for the *N*-nitrosation of 24 secondary amines by *asym*-N_2O_3. Calculations performed at the B3LYP-D3/def2-TZVP (IEF-PCM:water) level of theory.

It is noteworthy that the aliphatic amines have lower activation energies than the aromatic amines which may relate to the nucleophilicity of the amine. However, since acidic conditions are required to generate the active nitrosation species, whilst most of the amine will be protonated rather than in their free base form, rendering it inactive to nitrosation. This will interfere with the observed rate of reactivity of the *N*-nitrosation reaction.

The concentration of the free base will be dependent on its pK_a (the lower the pK_a the higher the concentration). For instance, it is expected the concentration of the active free base for *N*-methylaniline (pK_a = 4.85) [36] to be higher than the concentration of the free base for DMA (pK_a = 10.92) [37] which would result in a faster reaction for *N*-methylaniline, considering only the concentration factor. In contrast, *N*-methylaniline (10.34 kcal mol^{-1}) has a higher activation energy than DMA (2.97 kcal mol^{-1}), making DMA more reactive than *N*-methylaniline. Therefore, the actual reaction rate will depend on both, the pK_a and the activation energy.

The fraction of the free base for an amine with single pK_a can be calculated according to equation 1 [14]:

$$single\ pK_a\ fraction\ of\ free\ base = \frac{\frac{K_a}{[H^+]}}{1 + \frac{K_a}{[H^+]}} = \frac{K_a}{[H^+] + K_a} \qquad (1)$$

The rate constant k and the activation energy $\Delta G^{\ddagger}$ of a reaction is correlated in the Eyring equation (equation 2):

$$k = \frac{k_b T}{h} e^{\frac{-\Delta G^{\ddagger}}{RT}} \qquad (2)$$

The rate equation for the *N*-nitrosation reaction by N_2O_3 can be expressed as below (equation 3) [15]:

$$rate = k_{obs}[HNO_2]^2[R_2NH] \; where \; k_{obs} = \; k_{N_2O_2} x \; K_{N_2O_2} \qquad (3)$$

In the equation 3, the observed rate constant (k_{obs}) is composed by the second-order rate constant for nitrosation of the amine when N_2O_3 (k_{N2O3}) is the nitrosating agent and the equilibrium constant for the formation of N_2O_3 (K_{N2O3}) [15].

If we consider that the concentration of R_2NH is the fraction of free base of the amine ([DMA] = 1.2×10^{-8} and [*N*-methylaniline] = 1.39×10^{-2} in pH = 3, calculated according to equation 1). The κ_{N2O3} is the rate constant (κ_{DMA} and $\kappa_{N\text{-methylaniline}}$) calculated according to equation 2 using the $\Delta G^{\ddagger}$ value from the DFT calculation result ($\Delta G^{\ddagger}_{DMA}$ = 2.97 kcal mol^{-1} and $\Delta G^{\ddagger}_{N\text{-methylaniline}}$ = 10.34 kcal mol^{-1}). The reaction rate ratio for the *N*-nitrosation of *N*-methylaniline and DMA is 4.6 (equation 4). Thus, *N*-methylaniline is likely to react faster than DMA which is in accordance with experimental results [15].

$$\frac{rate_{N-\text{methylaniline}}}{rate_{DMA}} = \frac{K_{N_2O_3}\, k_{N-\text{methylaniline}}\, [HNO_2]^2\, [N\text{–}methylaniline]}{K_{N_2O_3}\, k_{DMA}\, [HNO_2]^2\, [DMA]} = 4.6 \qquad (4)$$

The results demonstrated the calculated activation energy affects the reactivity of the reaction however it does not directly correlate with the experimental constant rates as the reaction is also dependent on the pK_a of the amine.

Moreover, this study indicates that nitrosamines are very likely to form when secondary amines are exposed to nitrite in acidic conditions. Considering that nitrites are frequently found in excipients [38], one approach to address the risk is the use of scavengers. The scavengers can remove nitrite impurities from the drug formulation, thereby reducing the likelihood of *N*-nitrosamine formation [39]. Some potential scavengers for nitrite have been studied and the use of *p*-aminobenzoic acid (PABA) has demonstrated good results for *N*-nitrosamine inhibition [40, 41]. PABA is a primary amine that reacts with nitrite giving an unstable primary *N*-nitrosamine and, consequently, rapidly degrades to the corresponding diazonium ion (**Scheme 2**).

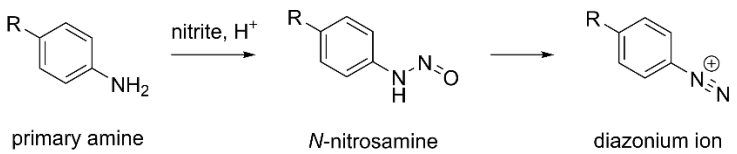

primary amine *N*-nitrosamine diazonium ion

PABA: R = CO_2H
Aniline: R = H

Scheme 2. Degradation of a primary amine to the diazonium ion.

DFT calculations were performed to gain more insight about the action of PABA as a scavenger. The energies of the reactants PABA + *asym*-N_2O_3, the transition state **TS-29**, the nitrosated PABA (NO-PABA) and the 4-carboxybenzenediazonium were calculated and depicted in **Figure 8**. The activation energy for the *N*-nitrosation step (18 kcal mol^{-1}) is high compared to most of the activation energies (1.97-18.76 kcal mol^{-1}) for the secondary amines calculated previously (**Figure *7***). However, the free energy for the whole process from the reactants PABA + *asym*-N_2O_3 to the product 4-carboxybenzenediazonium is considerably high (-50.8 kcal mol^{-1}) and therefore thermodynamically very favourable, thus drives the reaction towards the product. In addition, the calculations were also performed for aniline to assess the influence of the presence of the carboxylic acid in the aromatic ring of PABA. The results demonstrated similar but lower overall energy in the energy profile, showing an activation energy of 14.0 kcal mol^{-1} from reactants aniline + *asym*-N_2O_3 to the transition state **TS-30** and free energy of -59.0 kcal mol^{-1} from reactants aniline + *asym*-N_2O_3 up to the product benzenediazonium.

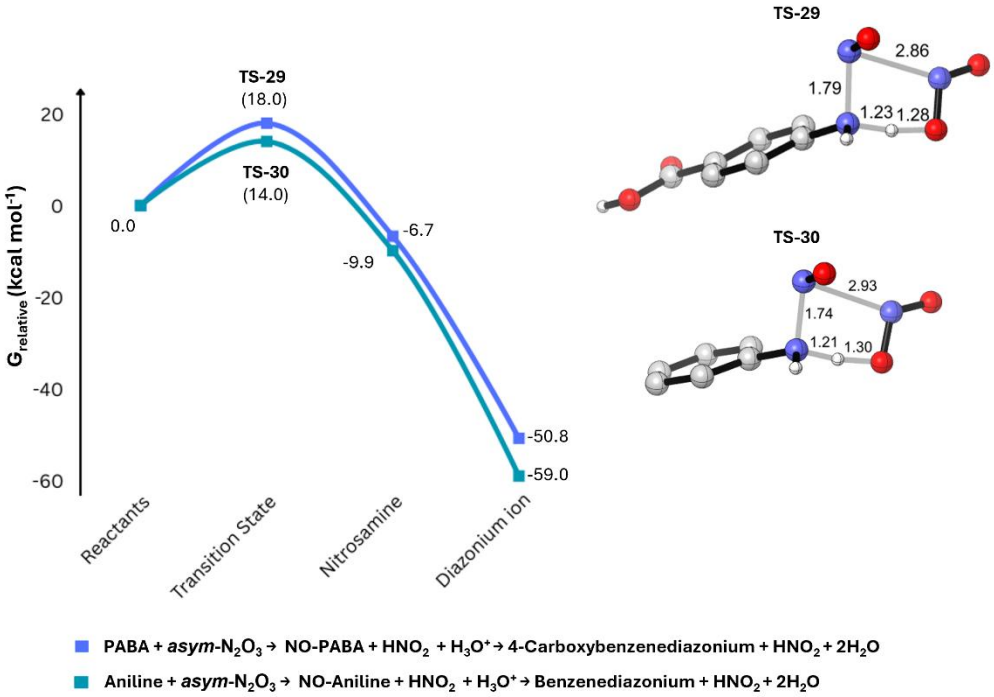

Figure 8. Gibbs free energy (G) profile of the *N*-nitrosation of PABA and aniline by *asym*-N_2O_3 at the B3LYP-D3/def2-TZVP (IEF-PCM:water) level of theory. Bond lengths are shown in Å.

Finally, two complex secondary amines were investigated, the API varenicline and the sitagliptin impurity (TTP) to evaluate the energy profile for the *N*-nitrosation reaction (**Scheme 3**).

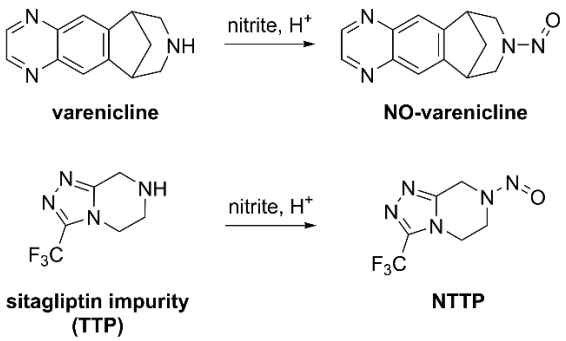

Scheme 3. *N*-Nitrosation of varenicline and sitagliptin impurity (TTP).

The energies of the reactants, transition states (**TS-31** and **TS-32)** and the nitrosated products (NO-varenicline and NTTP) were calculated (**Figure 9**). Varenicline showed lower activation energy (2.5 kcal mol^{-1}) than TTP (10.2 kcal mol^{-1}) and therefore, it is more reactive towards nitrosation. However, as demonstrated previously, the pK_a of the amine also plays a role and needs to be taken in consideration. The relative low activation energy suggests that both amines undergo facile nitrosation, which aligns to their reporting as nitrosamine drug substance-related impurities [42, 43].

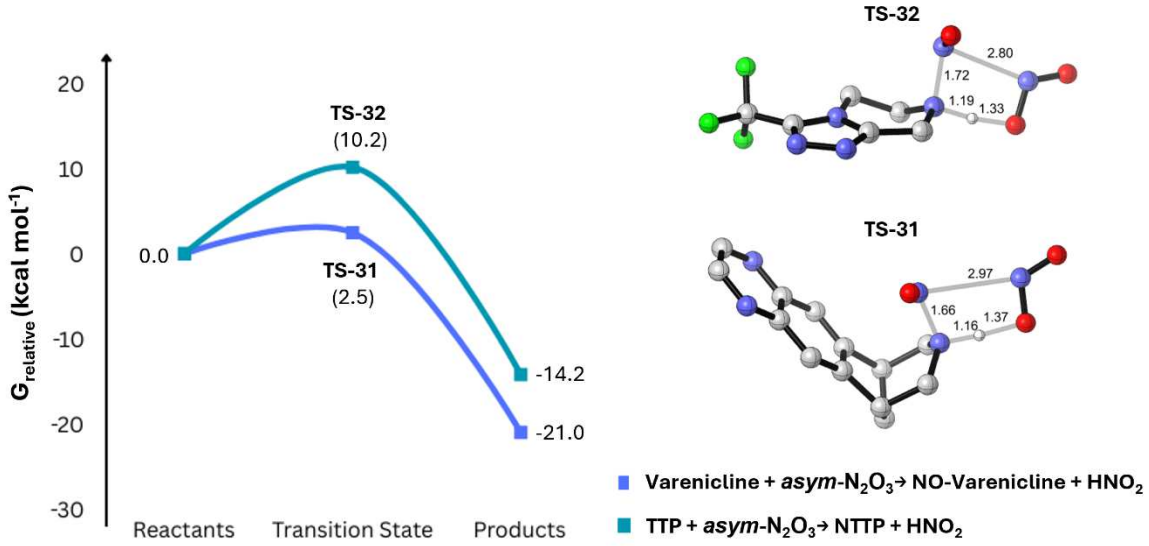

Figure 9. Gibbs free energy (G) profile of the *N*-nitrosation of varenicline and the degradant of sitagliptin by *asym*-N_2O_3 at the B3LYP-D3/def2-TZVP (IEF-PCM:water) level of theory. Bond lengths are shown in Å.

Conclusions

The energy profile for the *N*-nitrosation reaction of DMA, considering *asym*-N_2O_3, *sym*-N_2O_3, *trans-cis*-N_2O_3, NOCl, and HNO_2, was investigated using DFT. The *asym*-N_2O_3 was found to be the favourable species and was therefore used to evaluate the steric and electronic effects for 24 secondary amines.

The results for aliphatic amines demonstrated that steric hindrance increases the activation energy of the reaction, although the barrier is still very low (2-10 kcal mol^{-1}), suggesting that the reaction will

predominantly be encounter-controlled. Aromatic amines and amines bearing electron-withdrawing groups directly attached to the nitrogen atom have relatively higher activation energy (7-18 kcal mol^{-1}) compared to aliphatic amines and are therefore less reactive. However, the availability of the active free base is significantly higher in acidic media due to their lower pKa, resulting in an increased reaction rate.

Additionally, the mechanism by which the scavenger PABA captures nitrites was investigated, demonstrating the reaction is thermodynamically very favourable to the formation of the diazonium ion, presenting a free energy of -59.0 kcal mol^{-1}. The activation energies for varenicline and the sitagliptin impurity (TTP) were also calculated, showing low barriers of 2.5 kcal mol^{-1} and 10.2 kcal mol^{-1}, respectively. These low activation energies suggest that nitrosation is likely to occur for these pharmaceutical compounds.

Within the context of pharmaceuticals, the apparent lack of a significant barrier for the nitrosation of secondary amines across a range of steric and electronic influences indicates the formation of nitrosamines during manufacture and storage remains a credible risk irrespective of the amine structure. Risk assessments for demonstrating pharmaceutical safety will therefore rely on control of the contributing species (amines and nitrite) and/or efforts to define the kinetics of diffusion within drug product formulation to understand the long term risk of nitrosamine formation.

Acknowledgements

The authors would like to acknowledge Samuel Boobier, Emma Pye and Roberta Drekener for their insightful discussions and for reviewing the manuscript.

Author contributions

M.Y.K., D.J.P., and M.J.B. conceived the study. M.J.B., D.J.P and C.G.B guided the development of the study. M.K. conducted the calculations and prepared the initial draft of the manuscript. All authors reviewed the manuscript.

Funding

The authors declare that no funding was received during the preparation of this manuscript.

References

1. Bharate SS (2021) Critical Analysis of Drug Product Recalls due to Nitrosamine Impurities. J Med Chem 64:2923–2936. https://doi.org/10.1021/acs.jmedchem.0c02120

2. Schlingemann J, Burns MJ, Ponting DJ, Martins Avila C, Romero NE, Jaywant MA, Smith GF, Ashworth IW, Simon S, Saal C, Wilk A (2023) The Landscape of Potential Small and Drug Substance Related Nitrosamines in Pharmaceuticals. Journal of Pharmaceutical Sciences 112:1287–1304. https://doi.org/10.1016/j.xphs.2022.11.013

3. Burns MJ, Ponting DJ, Foster RS, Thornton BP, Romero NE, Smith GF, Ashworth IW, Teasdale A, Simon S, Schlingemann J (2023) Revisiting the Landscape of Potential Small and Drug Substance

Related Nitrosamines in Pharmaceuticals. Journal of Pharmaceutical Sciences 112:3005–3011. https://doi.org/10.1016/j.xphs.2023.10.001

4. Cioc RC, Joyce C, Mayr M, Bream RN (2023) Formation of *N* -Nitrosamine Drug Substance Related Impurities in Medicines: A Regulatory Perspective on Risk Factors and Mitigation Strategies. Org Process Res Dev 27:1736–1750. https://doi.org/10.1021/acs.oprd.3c00153

5. Teasdale A (2023) Reflections on the Impact of Nitrosamine Drug Substance Related Impurities. Org Process Res Dev 27:1685–1686. https://doi.org/10.1021/acs.oprd.3c00286

6. Wichitnithad W, Nantaphol S, Noppakhunsomboon K, Rojsitthisak P (2023) An update on the current status and prospects of nitrosation pathways and possible root causes of nitrosamine formation in various pharmaceuticals. Saudi Pharmaceutical Journal 31:295–311. https://doi.org/10.1016/j.jsps.2022.12.010

7. Nitrosamine impurities: guidance for marketing authorisation holders, European Medicines Agency, 2024. https://www.ema.europa.eu/en/human-regulatory-overview/post-authorisation/pharmacovigilance-post-authorisation/referral-procedures-human-medicines/nitrosamine-impurities/nitrosamine-impurities-guidance-marketing-authorisation-holders (accessed Feb 24, 2025)

8. Nitrosamine impurities in medications: Guidance, Health Canada, 2022. https://www.canada.ca/en/health-canada/services/drugs-health-products/compliance-enforcement/information-health-product/drugs/nitrosamine-impurities/medications-guidance.html (accessed Feb 24, 2025)

9. Control of Nitrosamine Impurities in Human Drugs: Guidance for Industry, U.S. Food and Drug Administration, 2020. https://www.fda.gov/regulatory-information/search-fda-guidance-documents/control-nitrosamine-impurities-human-drugs (accessed Feb 24, 2025)

10. Ashworth IW, Curran T, Dirat O, Zheng J, Whiting M, Lee D (2023) A Consideration of the Extent That Tertiary Amines Can Form *N* -Nitroso Dialkylamines in Pharmaceutical Products. Org Process Res Dev 27:1714–1718. https://doi.org/10.1021/acs.oprd.3c00073

11. Williams DLH (2004) Nitrosation reactions and the chemistry of nitric oxide, 1st ed. Elsevier, Amsterdam ; Boston

12. López-Rodríguez R, McManus JA, Murphy NS, Ott MA, Burns MJ (2020) Pathways for *N* -Nitroso Compound Formation: Secondary Amines and Beyond. Org Process Res Dev 24:1558–1585. https://doi.org/10.1021/acs.oprd.0c00323

13. Beard JC, Swager TM (2021) An Organic Chemist's Guide to *N* -Nitrosamines: Their Structure, Reactivity, and Role as Contaminants. J Org Chem 86:2037–2057. https://doi.org/10.1021/acs.joc.0c02774

14. Ashworth IW, Dey D, Dirat O, McDaid P, Lee D, Moser J, Nanda KK (2023) Formation of Dialkyl-*N* -nitrosamines in Aqueous Solution: An Experimental Validation of a Conservative Predictive Model and a Comparison of the Rates of Dialkyl and Trialkylamine Nitrosation. Org Process Res Dev 27:1759–1766. https://doi.org/10.1021/acs.oprd.2c00366

15. Ashworth IW, Dirat O, Teasdale A, Whiting M (2020) Potential for the Formation of *N* -Nitrosamines during the Manufacture of Active Pharmaceutical Ingredients: An Assessment of

the Risk Posed by Trace Nitrite in Water. Org Process Res Dev 24:1629–1646. https://doi.org/10.1021/acs.oprd.0c00224

16. Wang X, Zheng Q, Fan K (1997) Ab initio study on the structure and vibrational spectra of dinitrogen trioxide and its isomers. Journal of Molecular Structure 403:245–251. https://doi.org/10.1016/S0022-2860(96)09353-2

17. Lee C-I, Lee Y-P, Wang X, Qin Q-Z (1998) Isomers of N2O3: Observation of *trans-cis* N2O3 in solid Ar. The Journal of Chemical Physics 109:10446–10455. https://doi.org/10.1063/1.477700

18. Sun Z, Liu YD, Lv CL, Zhong RG (2009) Theoretical investigation of the isomerization of N2O3 and the N-nitrosation of dimethylamine by asym-N2O3, sym-N2O3, and trans–cis N2O3 isomers. Journal of Molecular Structure: THEOCHEM 908:107–113. https://doi.org/10.1016/j.theochem.2009.05.012

19. Sun Z, Liu YD, Zhong R (2011) Theoretical investigation of reactivities of amines in the N-nitrosation reactions by N2O3. J Mol Model 17:669–680. https://doi.org/10.1007/s00894-010-0750-4

20. Casado J, Castro A, Lorenzo FM, Meijide F (1986) Kinetic studies on the formation of N-nitroso compounds XI. Nitrosation of dimethylamine by nitrite esters in aqueous basic media. Monatsh Chem 117:335–344. https://doi.org/10.1007/BF00816527

21. Casado J, Castro A, Quintela MAL, Tato JV (1981) Kinetic Studies on the Formation of N-Nitroso Compounds. Zeitschrift für Physikalische Chemie 127:179–192. https://doi.org/10.1524/zpch.1981.127.2.179

22. Casado J, Castro A, Leis JR, Quintela MAL, Mosquera M (1983) Kinetic Studies on the Formation of N-Nitroso Compounds VI. The Reactivity of N203 as a Nitrosating Agent. Monatshefte für Chemie - Chemical Monthly 114:639–646

23. Mirvish SS (1975) Formation of N-nitroso compounds: Chemistry, kinetics, and in vivo occurrence. Toxicology and Applied Pharmacology 31:325–351. https://doi.org/10.1016/0041-008X(75)90255-0

24. Gaussian 16, Revision C.01, M. J. Frisch, G. W. Trucks, H. B. Schlegel, G. E. Scuseria, M. A. Robb, J. R. Cheeseman, G. Scalmani, V. Barone, G. A. Petersson, H. Nakatsuji, X. Li, M. Caricato, A. V. Marenich, J. Bloino, B. G. Janesko, R. Gomperts, B. Mennucci, H. P. Hratchian, J. V. Ortiz, A. F. Izmaylov, J. L. Sonnenberg, D. Williams-Young, F. Ding, F. Lipparini, F. Egidi, J. Goings, B. Peng, A. Petrone, T. Henderson, D. Ranasinghe, V. G. Zakrzewski, J. Gao, N. Rega, G. Zheng, W. Liang, M. Hada, M. Ehara, K. Toyota, R. Fukuda, J. Hasegawa, M. Ishida, T. Nakajima, Y. Honda, O. Kitao, H. Nakai, T. Vreven, K. Throssell, J. A. Montgomery, Jr., J. E. Peralta, F. Ogliaro, M. J. Bearpark, J. J. Heyd, E. N. Brothers, K. N. Kudin, V. N. Staroverov, T. A. Keith, R. Kobayashi, J. Normand, K. Raghavachari, A. P. Rendell, J. C. Burant, S. S. Iyengar, J. Tomasi, M. Cossi, J. M. Millam, M. Klene, C. Adamo, R. Cammi, J. W. Ochterski, R. L. Martin, K. Morokuma, O. Farkas, J. B. Foresman, and D. J. Fox, Gaussian, Inc., Wallingford CT, 2019

25. Becke AD (1993) Density-functional thermochemistry. III. The role of exact exchange. The Journal of Chemical Physics 98:5648–5652. https://doi.org/10.1063/1.464913

26. Stephens PJ, Devlin FJ, Chabalowski CF, Frisch MJ (1994) Ab Initio Calculation of Vibrational Absorption and Circular Dichroism Spectra Using Density Functional Force Fields. J Phys Chem 98:11623–11627. https://doi.org/10.1021/j100096a001

27. Kim K, Jordan KD (1994) Comparison of Density Functional and MP2 Calculations on the Water Monomer and Dimer. J Phys Chem 98:10089–10094. https://doi.org/10.1021/j100091a024

28. Weigend F, Ahlrichs R (2005) Balanced basis sets of split valence, triple zeta valence and quadruple zeta valence quality for H to Rn: Design and assessment of accuracy. Phys Chem Chem Phys 7:3297. https://doi.org/10.1039/b508541a

29. Grimme S, Antony J, Ehrlich S, Krieg H (2010) A consistent and accurate *ab initio* parametrization of density functional dispersion correction (DFT-D) for the 94 elements H-Pu. The Journal of Chemical Physics 132:154104. https://doi.org/10.1063/1.3382344

30. Cancès E, Mennucci B, Tomasi J (1997) A new integral equation formalism for the polarizable continuum model: Theoretical background and applications to isotropic and anisotropic dielectrics. The Journal of Chemical Physics 107:3032–3041. https://doi.org/10.1063/1.474659

31. Tomasi J, Mennucci B, Cancès E (1999) The IEF version of the PCM solvation method: an overview of a new method addressed to study molecular solutes at the QM ab initio level. Journal of Molecular Structure: THEOCHEM 464:211–226. https://doi.org/10.1016/S0166-1280(98)00553-3

32. GaussView, Version 6.1.1, Roy Dennington, Todd Keith, and John Millam, Semichem Inc., Shawnee Mission, KS, 2019

33. CYLview, 1.0b; Legault, C. Y., Université de Sherbrooke, 2009 (http://www.cylview.org)

34. Bibart CH, Ewing GE (1974) Vibrational spectrum of gaseous N2O3. The Journal of Chemical Physics 61:1293–1299. https://doi.org/10.1063/1.1682052

35. Bradley GM, Siddall W, Strauss HL, Varetti EL (1975) Infrared studies of asymmetrical dinitrogen trioxide. J Phys Chem 79:1949–1953. https://doi.org/10.1021/j100585a013

36. Bacarella AL, Grunwald E, Marshall HP, Purlee EL (1955) The Potentiometric Measurement of Acid Dissociation Constants and pH in the System Methanol-Water. pKa Values for carboxylic Acids and Anilinium Ions. J Org Chem 20:747–762. https://doi.org/10.1021/jo01124a007

37. Christensen JJ, Izatt RM, Wrathall DP, Hansen LD (1969) Thermodynamics of proton ionization in dilute aqueous solution. Part XI. pK, ΔH°, and ΔS° values for proton ionization from protonated amines at 25°. J Chem Soc A 0:1212–1223. https://doi.org/10.1039/J19690001212

38. Boetzel R, Schlingemann J, Hickert S, Korn C, Kocks G, Luck B, Blom G, Harrison M, François M, Allain L, Wu Y, Bousraf Y (2023) A Nitrite Excipient Database: A Useful Tool to Support N-Nitrosamine Risk Assessments for Drug Products. Journal of Pharmaceutical Sciences 112:1615–1624. https://doi.org/10.1016/j.xphs.2022.04.016

39. Bayne A-CV, Misic Z, Stemmler RT, Wittner M, Frerichs M, Bird JK, Besheer A (2023) N-nitrosamine Mitigation with Nitrite Scavengers in Oral Pharmaceutical Drug Products. Journal of Pharmaceutical Sciences 112:1794–1800. https://doi.org/10.1016/j.xphs.2023.03.022

40. Homšak M, Trampuž M, Naveršnik K, Kitanovski Z, Žnidarič M, Kiefer M, Časar Z (2022) Assessment of a Diverse Array of Nitrite Scavengers in Solution and Solid State: A Study of Inhibitory Effect on the Formation of Alkyl-Aryl and Dialkyl N-Nitrosamine Derivatives. Processes 10:2428. https://doi.org/10.3390/pr10112428

41. Kako Y, Toyoda Y, Hatanaka Y, Suwa Y, Nukaya H, Nagao M (1992) Inhibition of mutagenesis by p-aminobenzoic acid as a nitrite scavenger. Mutation Research Letters 282:119–125. https://doi.org/10.1016/0165-7992(92)90084-U

42. FDA Updates and Press Announcements on Nitrosamine in Varenicline (Chantix), U.S. Food and Drug Administration, 2022. https://www.fda.gov/drugs/drug-safety-and-availability/fda-updates-and-press-announcements-nitrosamine-varenicline-chantix (accessed Feb 24, 2025)

43. FDA works to avoid shortage of sitagliptin following detection of nitrosamine impurity, U.S. Food and Drug Administration, 2022. https://www.fda.gov/drugs/drug-safety-and-availability/fda-works-avoid-shortage-sitagliptin-following-detection-nitrosamine-impurity (accessed Feb 24, 2025)

Supplementary Files

This is a list of supplementary files associated with this preprint. Click to download.

- SupplementaryInformation.pdf